Biophysical Chemistry, 45 (1992) 41–50
Elsevier Science Publishers B.V., Amsterdam

BIOCHE 01696

Rotamer interconversion and its influence on the fluorescence decay of tyrosine: A molecular dynamics study

A.J. Kungl

Institut für Physikalische Chemie der Universität Wien, Währingerstrasse 42, A-1090 Wien (Austria)

(Received 23 December 1991; accepted in revised form 15 June 1992)

Abstract

To test the hypothesis of charge-transfer quenching between an electrophile in the alanyl sidechain (carbonyl carbon or protonated amino group) and the excited aromatic phenol-subunit, which leads to a bi-exponential fluorescence decay of tyrosine in acidic aqueous solution, we investigated the dynamics of this amino acid and of the peptide Gly–Tyr–Gly *in vacuo* and in water with classical molecular dynamics (MD) and with stochastic dynamics (SD) computer simulation. The proposed low-frequency of interconversions between sidechain rotamers on a fluorescence timescale could not be confirmed. Instead, frequent transitions for both, χ_1 and χ_2, dihedrals were observed. Simulating a low pH situation (protonated carboxylate group) did not significantly affect the transition frequency. Rotamer interconversions in the peptide Gly–Tyr–Gly, though significantly less, were also observed although the fluorescence decay of this compound could be described by a uni-modal lifetime distribution centered at 0.8 ns. The results obtained from simulations *in vacuo* and in solution were critically compared with those of stochastic simulations. We found the stochastic simulation in a better agreement to full MD (water explicitly included), which is highly time consuming, whereas the *in vacuo* simulations clearly deviated from both. We conclude from our results that, since the rotamers do frequently interconvert within the fluorescence lifetime of tyrosine, their contribution to the non-exponential fluorescence decay should be negligible.

Keywords: Molecular dynamics; Time-resolved fluorescence; Distributional analysis

1. Introduction

Molecular dynamics (MD) computer simulations have become a valuable tool in recent years for the investigation of rapid motions in (biological) macromolecules [1–3]. The improvements in time-resolved spectroscopy and the rapid increase of computing power have extended the time scale of both experiment and theory, so that some comparisons can already be made [4]. For example, time-resolved fluorescence anisotropy has contributed to the distinction of internal and overall motions in proteins, of which the former can also be studied by MD simulations since

Correspondence to: Max-Planck-Institut für Biochemie Abt. Strukturforschung, Am Klopferspitz, DW-8033 Martinsried, FRG. Phone: (089)8578-2702, Fax: (089)8578-3516, E-Mail: KUNGL@MPI782.BIOCHEM.MPG.DE.

sub-picosecond and picosecond time scales are regarded [5].

Because fluorescence of proteins results from intrinsic chromophores—the aromatic amino acids—it is of interest to get a molecular picture of their complex dynamics on fluorescence time scales. For this purpose one needs to regard a few nanoseconds, which is difficult to access numerically. Orientational fluctuations of tyrosine sidechains within a few picoseconds were used to study small amplitude motions in proteins [6]. Recently, Cartling investigated the long-time dynamics of proteins [7]. Commonly, fluctuations *in* conformational states are referred to as short-time dynamics, whereas sequences of transitions *between* conformational states belong to the long-time dynamics. The rates for conformational transitions were introduced as the basic parameters in a stochastic model of long-time dynamics [7]. Intramolecular motions of a chromophore can also be divided in the two described sub-classes. Short-time fluctuations of a fluorophore will not markedly influence its fluorescence lifetime. Whereas any significant change of the dipole direction (e.g. ring flip) and thus intense interaction with the surrounding medium may affect the electronic relaxation pattern. However, the dynamics can only be detected by time resolved fluorescence measurements when (a) the time scales of the deactivation (emission) and the dynamics can be compared and (b) fluorescence is sensitive to topological rearrangements (e.g. energy transfer, etc.).

A model has been suggested for the non-exponential fluorescence decay of the aromatic amino acids tyrosine [8,9] and tryptophan [10,11]. The so-called *rotamer model* proposes charge transfer quenching between the excited aromatic chromophore (an indole or a phenole ring, respectively) as donor and an electrophile in the alanyl sidechain (carbonyl carbon or protonated amino group) [11] as acceptor, depending on the relative position of the donor and acceptor, as is determined by the χ_1 and χ_2 dihedral angles within the sidechain (Fig. 1). χ_1 describes the relative orientation between the N–C^α–C^β plane and the C^α–C^β–C^γ plane and is measured clockwise around the C^α–C^β bond when viewed from

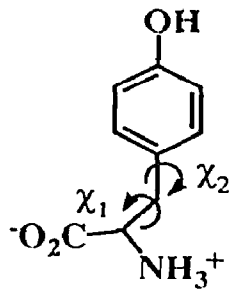

Fig. 1. χ_1 and χ_2 dihedrals in tyrosine.

C^α to C^β [12]. Whereas χ_2 describes the orientation of the C^α–C^β–C^γ plane relative to the C^β–C^γ–$C^{\delta 1}$ plane measured clockwise about the C^β–C^γ bond viewed from C^β to C^γ [12]. For a rigorous conformational analysis of aromatic amino acids by X-ray crystallography see [13].

Three energetically favored values were found for the χ_1 dihedral: g^-, t, g^+; and two were determined for the χ_2 dihedral: perpendicular (p) and antiperpendicular (ap) with respect to the aromatic plane [14]. Ground state conformational heterogeneity due to different rotamer populations in tyrosine was confirmed by ^{1}H NMR investigations [9]. Thus, intramolecular quenching can only lead to a non-exponential fluorescence decay when (a) the sidechain rotamers differ in their fluorescence lifetimes (assuming charge transfer) and (b) the corresponding rotamers do not (or at least very slowly) interconvert on a fluorescence time scale.

Engh et al. [15] have investigated the Brownian molecular dynamics of tryptophan. They found the χ_1 dihedral interconverting with a high frequency but not χ_2. They therefore proposed a modified rotamer model in which the two average values of χ_2, p and ap, which they found to be stable on a fluorescence time scale, account for the non-exponential fluorescence decay of tryptophan. Due to the chirality of the chromophore the authors suggested two different charge transfer channels according to the p and the ap configuration, respectively. However, their work did not include the influence of solvent explicitly, which may further enhance crossings of energetic barriers between distinct rotamers.

In the following we will demonstrate that for tyrosine in solution both χ_1 and χ_2 do interconvert frequently. We will further show that the influence of solvent should either be accounted for explicitly by computing the trajectories for a number of water molecules (full MD) or implicitly by integrating the Langevin equation of motion (SD). *In vacuo* simulations will be shown to pronouncedly deviate from these results. A tyrosine containing peptide (Gly–Tyr–Gly) was chosen to illustrate the influence of a peptide backbone on the transition rates in the χ_1 and χ_2 dihedrals. Conclusions will be drawn concerning the validity of the rotamer model for tyrosine fluorescence in molecular terms.

2. Fluorescence measurement and data analysis

Tyrosine and the peptide Gly–Tyr–Gly were purchased by Aldrich (Germany) and Bachem (Switzerland), respectively. For the fluorescence measurements, both substances were used without further purification.

Time-resolved fluorescence measurements were performed on a serial PRA 3000 transient configuration (Photochemical Research Association, Canada). The full width at half maximum of the thyratron-gated hydrogen flash-lamp was typically 1.5 ns. Fluorescence photons were detected by a Hamamatsu R928 photomultiplier and time-correlated by single photon counting [16].

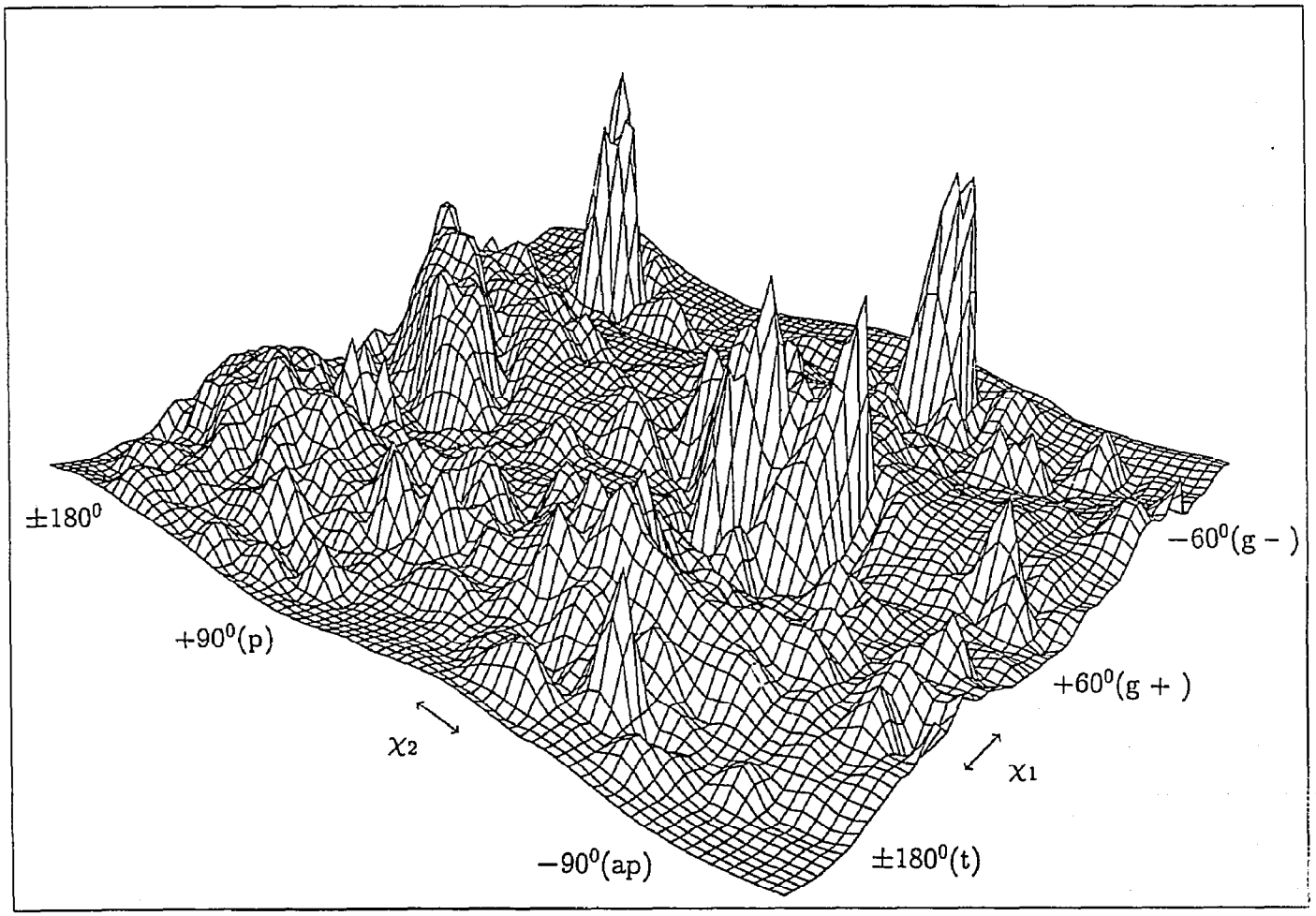

Fig. 2. Approximate potential energy surface for the tyrosine rotamers. The energy (z-axis) is plotted as a function of the χ_1/χ_2 dihedrals (x/y-axis, for further details see text).

The TAC-processed output signals were collected in a Tracor Northern TN 1750 multichannel analyzer.

A modified exponential series method (ESM) [17] was used to evaluate a potential distribution of fluorescence lifetimes from a (non-exponential) fluorescence response $F(t)$. In the ESM $F(t)$ is approximated by a series of exponentials with fixed lifetimes spaced equally or logarithmically over the time scale of fluorescence. From the convolution integral the corresponding set of amplitudes (distribution) is then evaluated in a linear, least-squares optimization. The method was shown to work well on high-accuracy synthetic and experimental data. No cut-off is required for deleting amplitudes of values close to zero during reconvolution. Contrary to other exponential series techniques our method is not restricted to positive amplitudes. Details of the method are given elsewhere [17].

3. Computational procedure

All the simulations were done using the GROMOS (GROningen MOlecular Simulation) program library. The molecular model and the force field are explicitly described in Ref. [18]. Initial conformations were generated from the X-ray structure of tyrosine by rotating the molecule about its unrestricted dihedrals. Rotamers with intrinsic torsional minima for χ_1 and χ_2 were taken in all possible combinations. Thus, six conformations were taken as the input for the dynamical simulations. The energy of the molecule was minimized using a steepest descents or a conjugate gradient algorithm (both included in GROMOS) with a final convergence criterion of an energy difference of 0.001 kJ/mol. Water was explicitly included according to the simple three-point charge (SPC) model of Berendsen et al. [19]. The initial conformations of the tripeptide Gly–Tyr–Gly were constructed using the program SYBYL (Tripos Ass.). Variations of the χ_1 and χ_2 dihedrals in the tyrosine unit were done according to their torsional minima.

A potential energy surface for the extended atom representation of the 17 atoms of tyrosine was generated (Fig. 2). For this purpose 36×36 configurations were generated by rotating the χ_1 and the χ_2 dihedrals. The three interatomic distances which specify the two dihedrals were restrained and the energy was then minimized for the remaining degrees of freedom with an energy difference convergence criterion of 0.001 kJ/mol. This value was taken as the grid point at the energy surface of the corresponding dihedrals.

In the dynamical simulations a potential energy typically applied to proteins was regarded [18], which describes the interaction between the atoms of the system. In the numerical integration of Newton's equation of motion the bond lengths were kept rigid by applying the SHAKE method [20] enabling a step size of 1 fs or longer. The temperature of the system was kept constant at $T_0 = 300$ K by coupling to a heat bath [21]. This was achieved by scaling the velocities v_i of all atoms according to a temperature relaxation time $\tau_T = 0.01$ ps. Periodic boundary conditions of a cubic box were applied. The cut-off radius for the long-range Coulomb force was taken to be 0.8 nm. The united atom approach was used in which the hydrogen atoms attached to carbon atoms were incorporated into the latter. Only polar hydrogens were treated explicitly. The simulation period was usually 100 ps for every input-conformation.

In the stochastic simulations (SD) the Langevin equation of motion

$$\frac{m_i \, \mathrm{d}v_i(t)}{\mathrm{d}t} = F_i(\{x_i\}) - m_i \gamma_i v_i(t) + R_i(t) \qquad (1)$$

was numerically integrated. The systematic force F_i must be derived from the interaction potential of mean force, the friction coefficient is denoted by γ_i, and the random force R_i is of white noise character, which is not correlated with prior velocities nor with the systematic force. The solvent friction coefficient for water was taken from Ref. [22] to be 91 ps^{-1}.

4. Results and discussion

In Fig. 2 an approximate potential energy surface for the two dihedrals χ_1 and χ_2 is shown.

Table 1

Parameters and results characterizing the simulations. The transitions were monitored within a time-span of 600 ps for each method. For further details see text

Dynamics	time-step (fs)	Σ atoms (avg.)	CPU-time [a]	$t \leftrightarrow g^-$	$g^- \leftrightarrow g^+$	$t \leftrightarrow g^+$	$p \leftrightarrow ap$
MD *in vacuo*	2	17	4	1	0	1	1
MD in water	1	117	90	9	5	0	14
SD [b]	2	17	4	8	1	0	8

[a] The CPU time is presented in minutes for 1 ps simulation on a VAX-Station 2000.
[b] The solvent friction coefficient was taken from Ref. [22] to be 91 ps^{-1}.

The characteristic features are three grooves of χ_1 values corresponding to the g^+ (60°), g^- (−60°), and the t (±180°) configuration (see also Fig. 1) and two grooves of the χ_2 values corresponding to the perpendicular (p, 90°) and the antiperpendicular (ap, −90°) configuration. Thus, six theoretical favorable configurations [14] are well represented. The plot also provides differences in the energetic barriers (ΔE_{barr}) between distinct rotamers. At minimum χ_2 values (p and ap) the lowest χ_1-barrier is between t and g^- (hydrogen eclipsed with the phenole ring, ΔE_{barr} ~ 15 kJ/mol), followed by a little higher barrier between g^+ and g^- (eclipsed ammonium group, ΔE_{barr} ~ 20 kJ/mol) and the highest barrier between t and g^+ (eclipsed carboxylate group, ΔE_{barr} ~ 40 kJ/mol). At minimum χ_1 values the barriers between the two favorable χ_2 values do not differ significantly (ΔE_{barr} ~ 25 kJ/mol). We would hence expect transitions between χ_1 dihedrals with a probability according to the energetic barrier between them and equally probable transitions between χ_2 dihedrals.

With the barrier results given above we estimated the transition rate constants for dihedral interconversion according to $k = \kappa \cdot \nu_T \exp(-\Delta E_{barr}/RT)$. The vibrational frequency at the bottom of the well ν_T was estimated [6] from the potential of mean force to be 2.5×10^{13} s^{-1}. Setting the transition state value for the transmis-

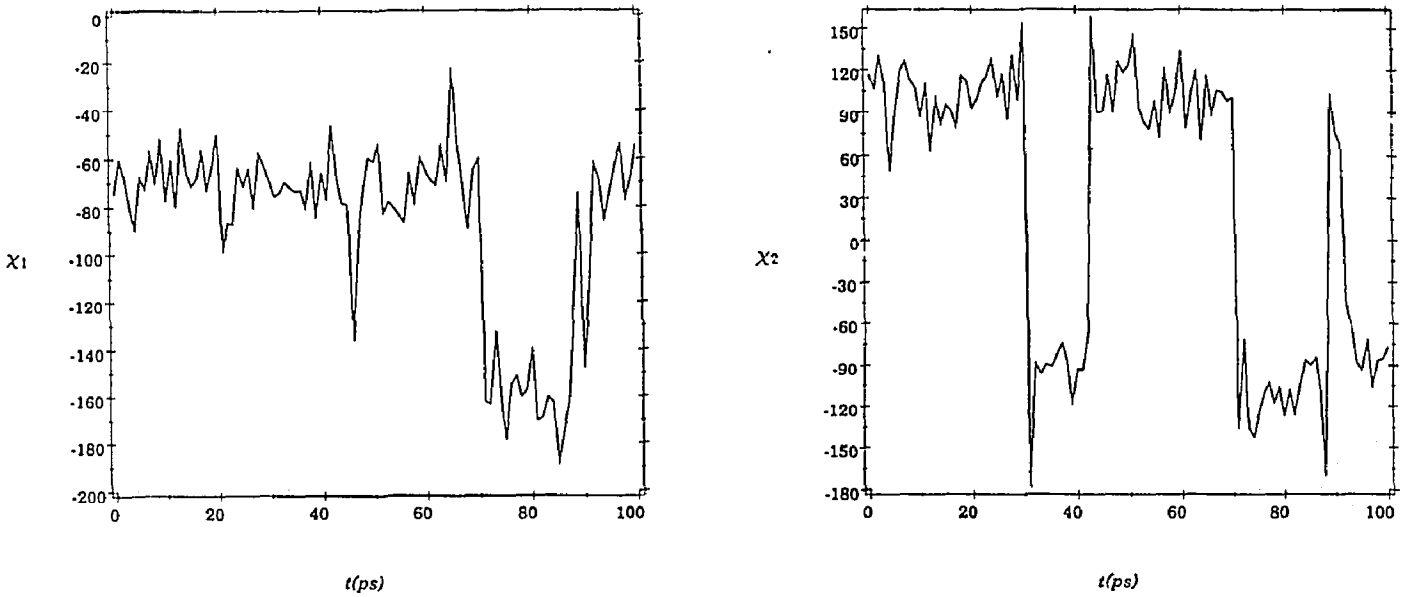

Fig. 3. Trajectories of the χ_1 and χ_2 interconversions demonstrating the frequency of these events. As initial configuration a g^-/p (−60°/90°) together with 96 molecules of water was chosen.

sion coefficient $\kappa \simeq 1$ we obtained upper limits for the transition rates: $k(p \leftrightarrow ap) \simeq 1.1 \times 10^9$ s^{-1}, $k(t \leftrightarrow g^-) \simeq 6.1 \times 10^{10}$ s^{-1}, $k(g^+ \leftrightarrow g^-) \simeq 8.2 \times 10^9$ s^{-1}, and $k(t \leftrightarrow g^+) \simeq 2.7 \times 10^6$ s^{-1}.

A total of three transitions was observed for tyrosine *in vacuo* during a simulation period of 600 ps at 300 K (see Table 1): two χ_1 transitions and one χ_2 transition (see Table 1) referring to average rotamer lifetimes of a few hundred picoseconds. Thus, energy barriers cannot easily be crossed. This is in quite good agreement with the transition rates given above. On the basis of classical MD *in vacuo*, therefore, a rotamer model for the non-exponential fluorescence decay of tyrosine seems possible with a slight preference given to the χ_2 model [15]. Nevertheless, a rotamer model, based on χ_2 non-interconverting dihedrals, cannot apply to the non-exponential fluorescence decay of tyrosine, since the two favorable configurations, p and ap, are in fact topologically identical (see, Fig. 1). Charge transfer to the side chain should evidently yield a single exponential decay. Whereas for tryptophan the p and the ap configuration differ due to the asymmetry of the chromophore. However, since the influence of the solvent on the dynamics of the chromophore should not be neglected, we have to estimate the rotamer lifetimes under the influence of the solvent, before judging the model for the fluorescence decay of aqueous tyrosine.

One hundred molecules of water were treated explicitly in each of the six full classical simulations of one tyrosine molecule in solution at 300 K (see Table 1). A smaller time step (1 fs) for the integration of the equations of motion was needed to account for the larger displacements compared with the *in vacuo* and SD simulations (time step: 2 fs). A total of 28 transitions was detected within 600 ps: 14 transitions in χ_1 and 14 transitions in χ_2 resulting in average lifetimes of 42 ps for the χ_1 as well as for the χ_2 rotamers. Typical trajectories for χ_1 and χ_2 transitions are shown in Fig. 3. The preferred paths for the transitions on the potential energy surface were found between $t \leftrightarrow g^-$ (see Table 1). Less transitions from $g^+ \leftrightarrow g^-$ and no transition from $t \leftrightarrow g^+$ (see Table 1) indicate the higher barriers between these rotamers. The incorporation of water molecules in the simulations obviously facilitates interconversions of *both* dihedrals. In addition to the equilibrium influence of solvation on the potential of tyrosine in solution, collisions of the chromophore with the solvent molecules should give rise to enhanced transitions of energetic barriers between distinct rotamers.

Thus, if water is explicitly regarded, approximate rotamer lifetimes of a few tens of picoseconds are found. Since the fluorescence lifetime of tyrosine in water at neutral pH (zwitterionic species) is about 3 ns (single exponential decay), the rotamers interconvert too fast to significantly influence the photophysics of the excited chromophore. Theoretically, we would hence expect the fluorescence decay of tyrosine to decay monoexponentially. This is in good agreement with the experiment at this pH. But at lower pH (protonated carboxylate group) the fluorescence decay of tyrosine is best described by two exponential terms [8,9]. The authors refer to a slowing of interconversions by the additional proton (respectively to a differential quenching due to the protonated α-carboxyl group) [9]. This proton, which has been incorporated explicitly in accompanied simulations, had no detectable influence on the interconversion rates (data not shown). SD simulations, for example, provided average lifetimes of 45 ps for χ_1 and 100 ps for χ_2 rotamers. Again, a χ_2 rotamer model cannot account for the bi-exponential decay (see above). A bigger substituent need to be considered for a more rigorous restriction of interconversions (see below).

Stochastic dynamics (SD) was also applied to the six input conformations of tyrosine. Within a total of 600 ps simulation period nine transitions in χ_1 and eight transitions in χ_2 were observed, resulting in an average rotamer lifetime of 66 ps for the χ_1 and 75 ps for the χ_2 rotamers. Nearly all χ_1 transitions occurred between $g^- \leftrightarrow t$ (see Table 1).

Obviously a SD simulation is a better approximation to a full MD simulation which treates water molecules explicitly. A reduction factor of 20 in the CPU time between SD and full MD clearly demonstrates the advantage of the former method, especially when larger systems, like proteins or DNA, are investigated. For tyrosine, these

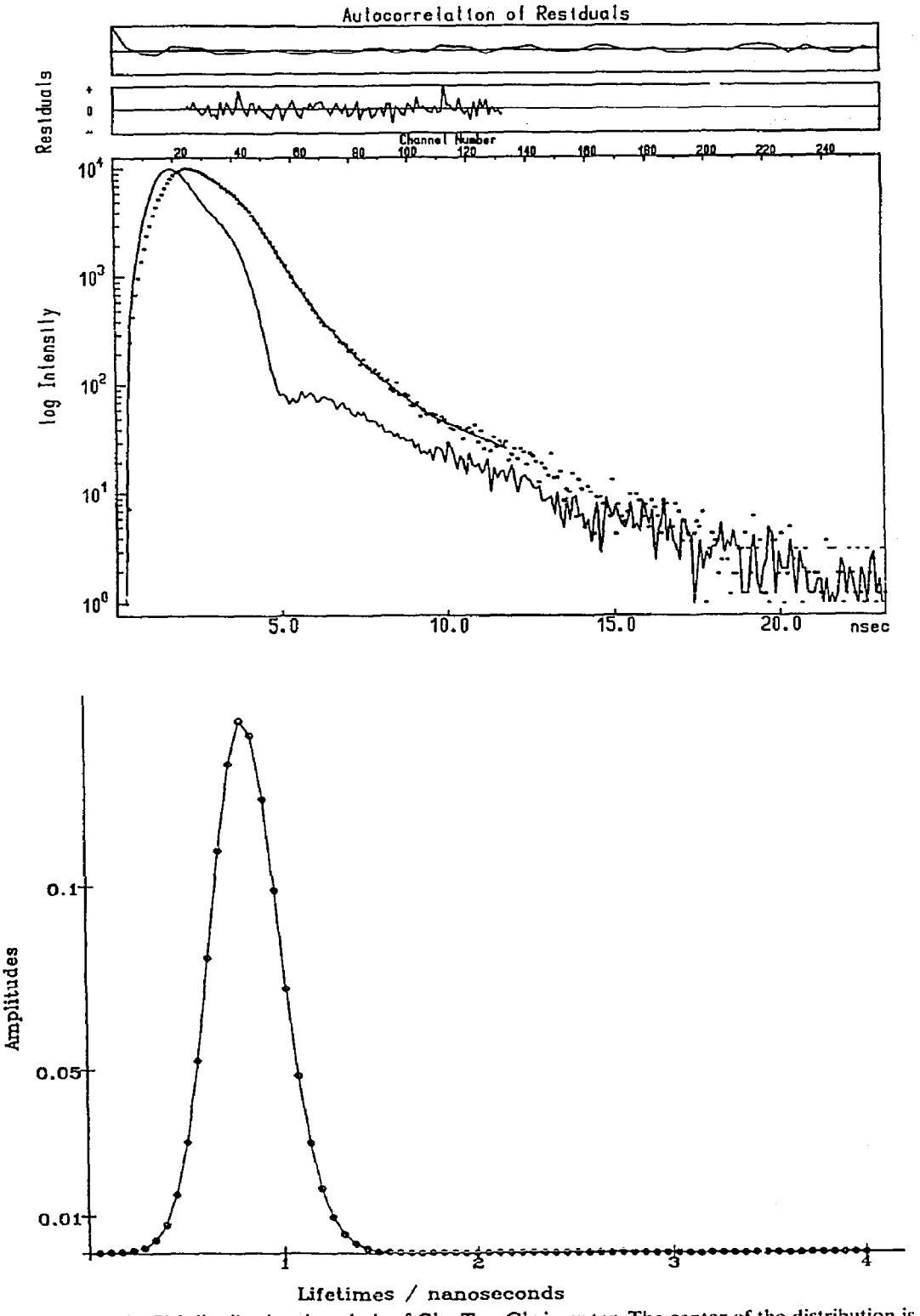

Fig. 4. Fluorescence decay and ESM distributional analysis of Gly–Tyr–Gly in water. The center of the distribution is located at 0.8 ns ($\chi^2 = 0.9$).

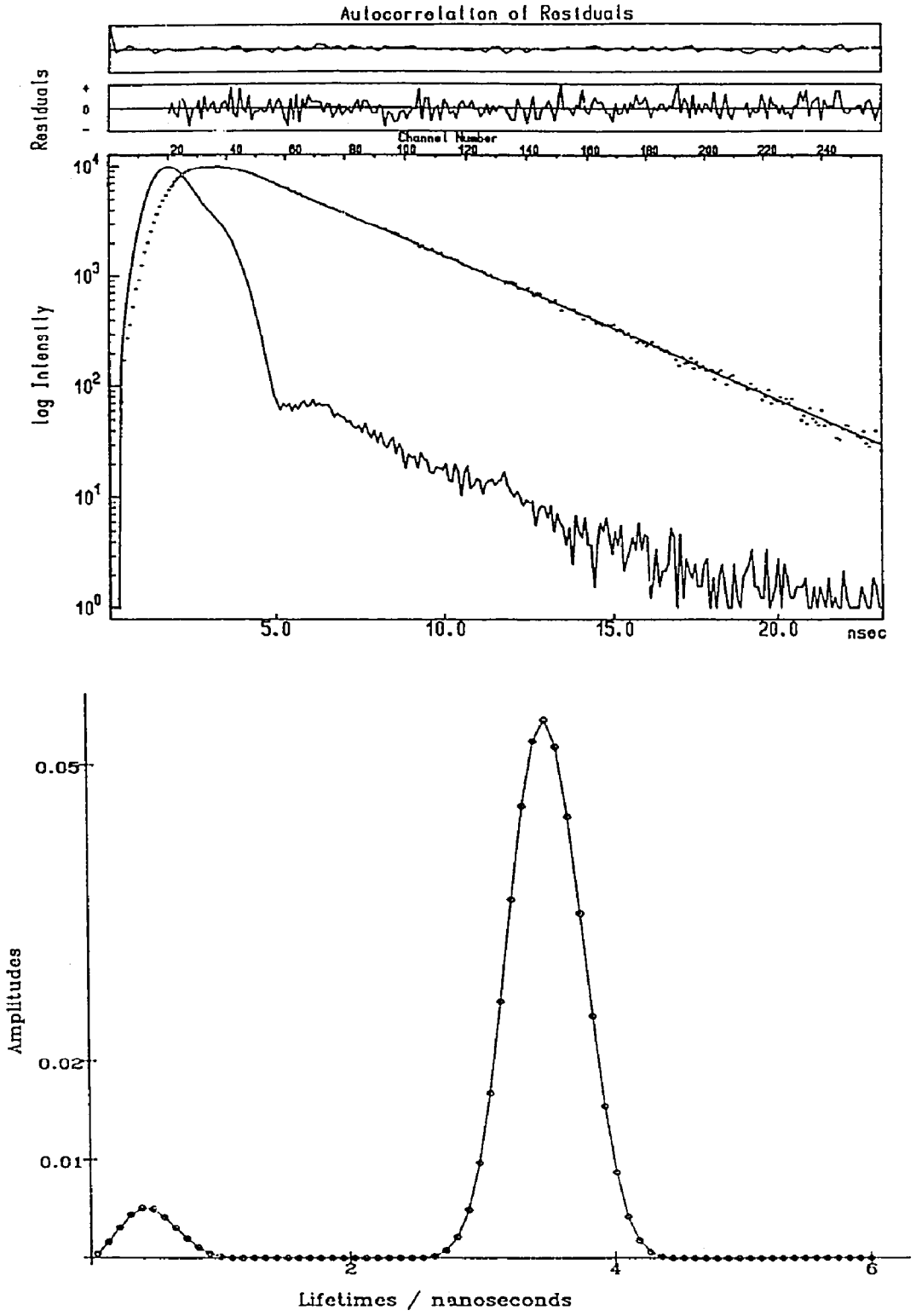

Fig. 5. Fluorescence decay and ESM distributional analysis of tyrosine in water. The centers of the distributions are located at 0.4 ns and 3.5 ns ($\chi^2 = 1.3$).

two methods show in accord frequent transitions of energy barriers between distinct rotamers when solvent is regarded in any form, implicitly (SD) or explicitly (full MD) against the results of MD *in vacuo*. However, the stochastic approach, although a significant improvement to *in vacuo* simulations, provides only 66% of the interconversions which the full MD can afford. This limited accuracy has to be kept in mind when SD is chosen because of its less computing expense.

To study the influence of a peptide backbone on the interconversion rates we computed the trajectories for the peptide Gly–Tyr–Gly. Again, classical MD (*in vacuo* and in water) was compared to SD. The number of water molecules included in the full MD simulations was increased to 170. Initial conformations of the interesting dihedrals were generated as described above for tyrosine. The peptide itself was regarded in an almost helical, sheet, and random configuration, respectively. Only the zwitterionic form of the molecule was simulated. Indeed, the transition rates were significantly affected by the glycyl substituents, resulting in average rotamer lifetimes of 100 ps for both χ_1 and χ_2 dihedrals in the tyrosine subunit. The two methods, full MD and SD, provided equivalent results as described above for tyrosine.

If the fluorescence of this peptide is regarded, one would thus expect the emission to decay at least bi-exponentially. In fact, we found this to be the case, but the two lifetimes were lying so closely together—0.5 ns and 0.9 ns—that they should be better described by one sharp lifetime distribution centered at 0.8 ns (Fig. 4). Whereas the lifetimes for tyrosine at pH < 3 are well separated at 0.4 ns and at 3.5 ns (Fig. 5). Since the interconversion rates of rotamers in Gly–Tyr–Gly are still fast compared with the fluorescence lifetime of this peptide, though they are slower compared with the interconversion rates of tyrosine one would expect average fluorescence lifetimes for both substances. This was shown to be true for the tyrosine-containing peptide (Fig. 4). However, the bi-exponential decay of tyrosine in acidic solution (Fig. 5) should lead to a more rigorous proof of the rotamer hypothesis.

5. Conclusions

Molecular dynamic simulations of tyrosine in water yielded transition frequencies which are not compatible with the rotamer model proposed for the bi-exponential fluorescence decay of tyrosine in acidic solution [8,9]. The time scale of rotamer interconversion ($\sim$ ps) is clearly seperated from the fluorescence time scale ($\sim$ ns) indicating temporal average contributions of different conformers to the intramolecular charge transfer. The rotamer model, moreover, is not able to correctly predict the fluorescence decay of the peptide Gly–Tyr–Gly. Since the influence of solvent has not been regarded explicitly in previous simulations [15], the central issue of this work was to compare different methods in order to recognize the magnitude of this influence. Water was found to be essential for dihedral interconversion in tyrosine. We may thus conclude that nanosecond time-resolved fluorometry—although sensible to conformational relaxation in proteins [23]—should not be sensible to rotamer interconversions in aqueous tyrosine. We suggest the role of solvent itself for the fluorescence decay of tyrosine to be the topic of future research.

Acknowledgements

I owe special thanks to Prof. W.F. van Gunsteren (ETH Zürich) for providing me with the program GROMOS and for giving me advice on the manuscript. I also thank Dr. A. Beyer, H. Schreiber and Prof. H. Kauffmann for numerous fruitful discussions. This work was supported by the Fonds zur Förderung der wissenschaftlichen Forschung, Vienna, Austria (Projekt: P7182).

References

1 C.L. Brooks, M. Karplus and B.M. Petit, Adv. Chem. Phys. LXXI (1988).
2 W.F. van Gunsteren and H.J.C. Berendsen, Angew. Chem. 29 (1990) 992.
3 J.A. McCammon and S.C. Harvey, Dynamics of proteins and nucleic acids (Cambridge Univ. Press, London, 1987).

4 L.X.-Q. Chen, R.A. Engh and G.R. Fleming, J. Phys. Chem. 92 (1988) 4811.
5 L.X.-Q. Chen, R.A. Engh, A.T. Brünger, D.T. Nguyen, M. Karplus and G.R. Fleming, Biochemistry 27 (1988) 6908.
6 J.A. McCammon, P.G. Wolynes and M. Karplus, Biochemistry 18 (1979) 927.
7 B. Cartling, J. Chem. Phys. 91 (1989) 427.
8 P. Gauduchon and P. Wahl, Biophys. Chem. 8 (1977) 87.
9 W.R. Laws, J.B.A. Ross, H.R. Wyssbrod, J.M. Beechem, L. Brand and J.C. Sutherland, Biochemistry 25 (1985) 599.
10 A.G. Szabo and D.M. Rayner, J. Am. Chem. Soc. 102 (1980) 554.
11 M.C. Chang, J.W. Petrich, D.B. McDonald and G.R. Fleming, J. Am. Chem. Soc. 105 (1983) 3819.
J.W. Petrich, M.C. Chang, D.B. McDonald and G.R. Fleming, J. Am. Chem. Soc. 105 (1983) 3824.
12 IUPAC-IUB Comission on Biochemical Nomenclature, J. Mol. Biol. 52 (1970) 1.
13 V. Cody, W.L. Duax and H. Hauptmann, Int. J. Peptide Protein Res. (1973) 297.
14 S.S. Zimmerman, M.S. Pottle, G. Nemethy and H.A. Scheraga, Macromolecules 10 (1977) 1.
15 R.A. Engh, L.X.-Q. Chen and G.R. Fleming, Chem. Phys. Lett. 126 (1986) 365.
16 D.V. O'Connor and D. Philips, Time-correlated single photon counting (Academic Press, London, 1984).
17 G. Landl, T. Langthaler, H.W. Engl, and H.F. Kauffmann, J. Comp. Phys. 95 (1991) 1.
18 W.F. van Gunsteren and H.J.C. Berendsen, Groningen Molecular Simulation (GROMOS) Library Manual (Biomos, Groningen, 1987).
19 H.J.C. Berendsen, J.P.M. Postma and W.F. van Gunsteren, in: Intermolecular forces, ed. P. Pullman (Reidel, Dordrecht, 1981) p. 331.
20 W.F. van Gunsteren and H.J.C. Berendsen, Mol. Phys. 34 (1977) 1311.
21 H.J.C. Berendsen, J.P.M. Postma, W.F. van Gunsteren, A. DiNola and J.R. Haak, J. Chem. Phys. 81 (1984) 3684.
22 S. Yun-Yu, W. Lu and W.F. van Gunsteren, Mol. Sim. 1 (1988) 369.
23 J.R. Alcala, E. Gratton and F.G. Prendergast, Biophys. J. 51 (1987) 597.